Label-Free Optical Sensing on Hybrid Plasmonic-Nanobiosilica Platforms

Fanghui Ren[1], Jeremy Campbell[2], Gregory L. Rorrer[2*], Alan X. Wang[1*]
[1]School of Electrical Engineering and Computer Science, Oregon State University, Corvallis, OR, 97331, USA;
[2]School of Chemical, Biological & Environmental Engineering, Oregon State University, Corvallis, OR, 97331, USA
*Corresponding authors: rorrergl@engr.orst.edu, wang@eecs.oregonstate.edu

ABSTRACT

Diatoms are single-celled algaes that make photonic-crystal-like silica shells or frustules with hierarchical micro- & nano-scale features consisting of two-dimensional periodic pores. In this paper, we present an innovative label-free optical sensor based on a biological-plasmonic hybrid nanostructure by self-assembling silver (Ag) nanoparticles into diatom frustules. The photonic-crystal-like diatom frustules provide a spatially confined electric field with enhanced intensity that can form hybrid photonic-plasmonic modes through the optical coupling with Ag nanoparticles. The experimental results demonstrate 4-6× and 9-12× improvement of sensitivities to detect the Raman dye for resonance and nonresonance SERS sensing, respectively.

Keywords: Diatom frustules, Raman mapping, guided mode resonance, localized surface plasmons.

1. INTRODUCTION

Inspired by advanced nanofabrication techniques, rationally designed plasmonic sensors have gained tremendous research interest in recent years [1-3]. Although unprecedented sensitivity, repeatability and specificity have been achieved, many of these rationally designed plasmonic sensors are manufactured using cost-prohibitive, top-down nanofabrication techniques and may not be feasibly used as disposable sensors for point-of-care applications [4-6]. Diatoms are photosynthetic micro-organisms that create their own skeletal shells of hydrated amorphous silica, called frustules, which naturally possess hierarchical micro- & nano-scale features [7-8]. These diatom nanostructures are readily and cheaply obtained by cultivation of diatom cells, followed by isolation of the diatom frustules through conventional chemical separation techniques, providing a cost-effective and scalable source of photonic crystal structures. In this paper, we theoretically and experimentally investigated the interactions between localized surface plasmons (LSPs) and guided-mode resonances (GMRs) by integrating silver (Ag) nanoparticles (NPs) onto diatom frustules. Numerical simulations indicate that the electric field (E-field) amplitude of LSPs can be significantly enhanced due to the coupling of the LSPs with the photonic structure of the diatom, especially when the Ag NPs are placed inside the pores of the frustules. By coating Ag NPs onto diatom frustules using a self-assembly method, we observed stronger optical scattering from the Ag NPs on diatom frustules than the Ag NPs on the glass substrate due to the LSPs. SERS detection of Rhodmine 6G (R6G) molecules at resonance wavelength (532 nm) shows that the NPs-on-diatom structure provides 4-6× improvement in sensitivity when compared to the NPs-on-glass structure that is confirmed by confocal SERS mapping. When excited by nonresonance wavelength (785nm), the NPs-on-diatom structure provides 9-12× improvement in SERS sensitivity.

2. THEORETICAL INVESTIGATION

2.1 Guided Mode Resonance of Diatom Frustules

The diatom frustules have regular arrays of sub-micron primary pores, which are lined with a thin layer of biosilica containing several nanopores with diameters below 100nm [9]. Simulations were conducted using a three-dimensional finite element method in RF module within Comsol 3.5a. The diatom frustule was modeled as a flat slab with a uniform thickness of 120 nm. Nanopores were modeled as cylindrical air holes with a unit pattern consisting of a central 50 nm pore surrounded by four 80 nm cylindrical pores, with a lattice constant of 450nm. A 10 × 10 array of unit cells, as

Frontiers in Biological Detection: From Nanosensors to Systems VI,
edited by Benjamin L. Miller, Philippe M. Fauchet, Brian T. Cunningham, Proc. of SPIE
Vol. 8933, 89330J · © 2014 SPIE · CCC code: 1605-7422/14/$18 · doi: 10.1117/12.2042429

shown in Fig. 1(a), was illuminated at normal incidence with a 5 μm Gaussian beam polarized in the x-direction. The refractive index of the slab was set to 1.46 for silicon dioxide.

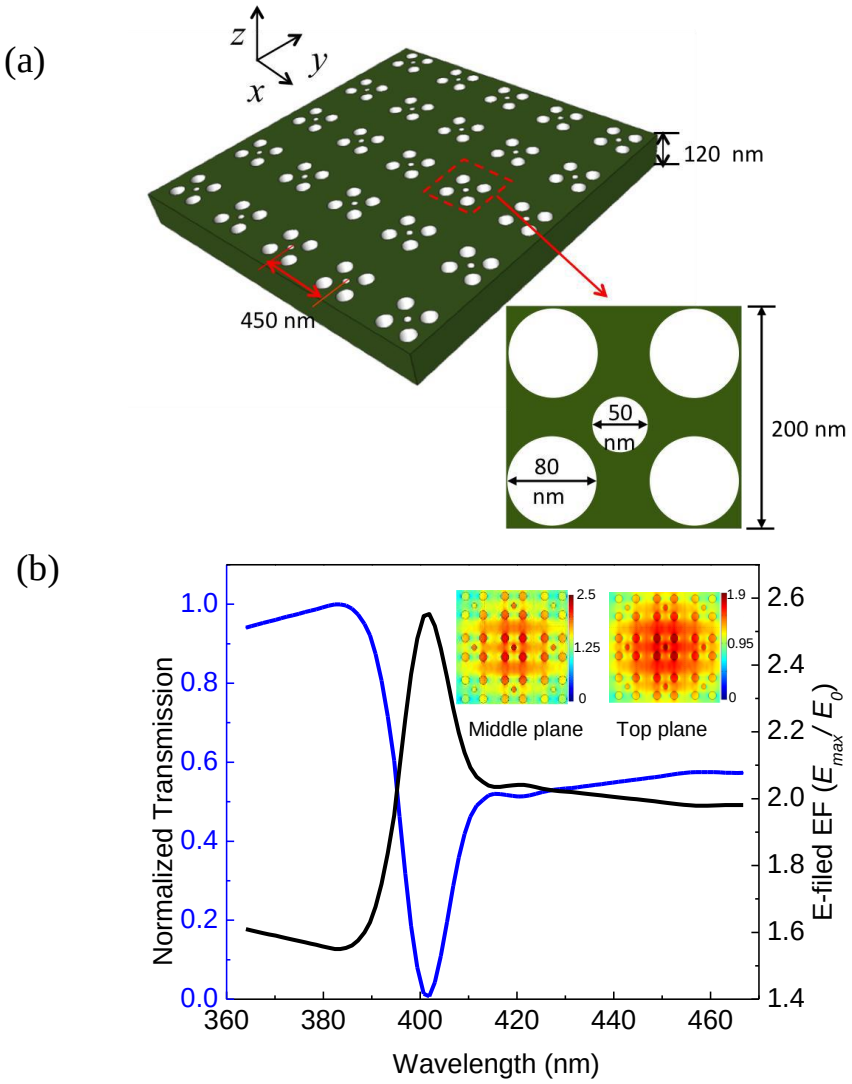

Fig.1. (a) Diatom frustule model with 2-D periodic unit cells. (b) Simulated normalized optical transmission (blue line) and E-field EF of the diatom frustule (black line).

From the simulated transmission spectrum shown in Fig. 1(b), the model exhibits a sharp resonance, which possesses a typical asymmetric shape around 10 nm wide at approximately 400 nm. It is attributed to the GMR effect which arises from coupling between the discrete guided modes of the photonic crystal slab and the radiation continuum above the light line. The E-field enhancement factor (EF) (E_{max}/E_0, where E_{max} is the maximum E-field amplitude inside the frustule and E_0 is the E-field amplitude of the incident Gaussian beam), is also plotted in Fig. 1(b). The inset figure shows E-field amplitude distribution in the middle plane and at the top surface of the diatom frustule with peak E-field EF of 2.5× and 1.87×, respectively. The maximum E-field EF is located at the middle plane of the photonic slab however E-field enhancement is still predicted at the slab surfaces.

2.2 Coupling Between GMRs and LSPs

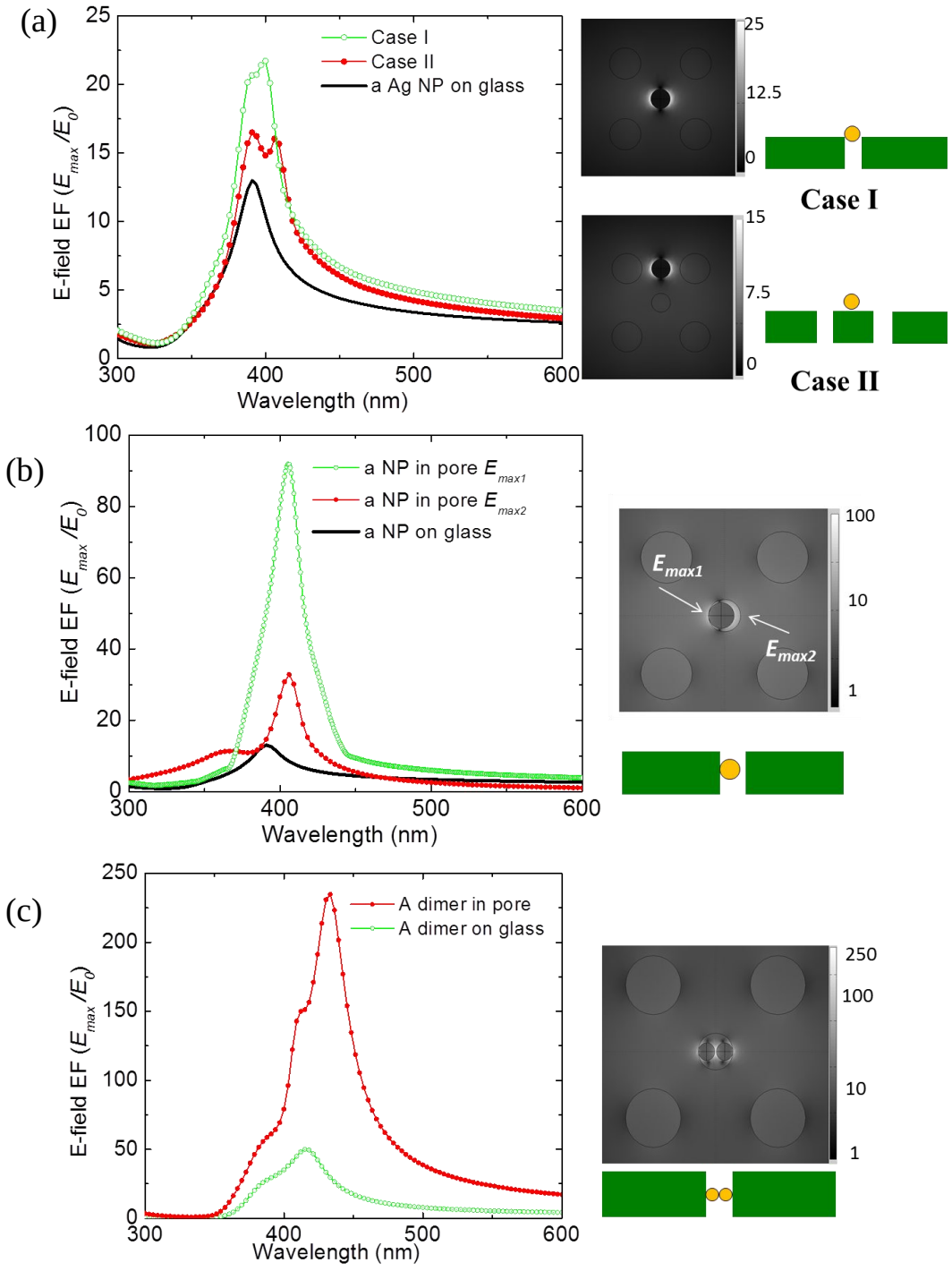

Figure 2. (a) the E-field EF and distribution of a "weak configuration", which is a single Ag NP on top of a diatom frustule. Case I and Case II correspond to different location of the Ag NP. (b) (c) the E-field EF and E-field distribution of a "strong configurations" , which shows a single Ag NP and a dimer inside the pore of a diatom frustule respectively. The field distributions of (b) (c) are in log scale.

To explore the interactions between the GMR effect of diatom frustules and LSPs of Ag NPs, we conduct further simulation by comparing two different configurations. In the first configuration, a single Ag NP is coated on top of the diatom frustule. Because the GMR and the LSPs are spatially separated, we call this configuration a "weakly" coupled system. While in the second configuration, the Ag NP is placed inside the pores to achieve a strong overlap between the GMR and LSPs, for which we call it as a "strongly" coupled system. Figure 2(a) shows the comparison of the maximum E-field EF of a 50nm Ag sphere NP on top of a glass substrate and on top of the diatom frustule surface, which represents the weakly coupled system. Two typical cases of the Ag NP positions with respect to the unit cell are considered: on top of the center air hole (case I), and on top of the frustule slab between the corner holes (case II). These positions are shown in the right panel of Fig. 2(a) together with the E-field distribution, respectively. The simulation results indicate that a stronger E-field EF is achievable when the Ag NP is placed on top of the central air hole, which is roughly improved by a factor of 1.8× compared with the same Ag NP on a glass substrate. Thus the total E-field enhancement of a weakly coupled system approximately equals to the product of the E-field EFs of the Ag NP and the diatom frustule. The E-field EFs of the other case is not as good as case I. We also observed that there are two distinct peaks in the resonant spectra of the Ag NP on the diatom frustule, where the first peak is the LSP of the Ag NP and the second is the GMR of the diatom frustule. These two resonant peaks are quite close to each other and can be barely identified.

In the second configuration, the Ag NPs are integrated inside the pores of the diatom frustules. Such configuration is experimentally feasible if the Ag NPs are smaller than the pores. For example, Figure 2 (b) shows the simulated E-field EF of a 40 nm Ag NP that is attached to the wall of the central pore. To achieve the strongest E-field, the Ag NP is aligned to the middle plane. The field profile of the single NP inside the pore becomes highly asymmetric as shown in the right part of Fig. 2(b). The peak E-field EF from the NP surface touching the wall (E_{max1}) is around 6× larger than that on a glass substrate, which is partially due to the higher dielectric constant of the surrounding material. Nevertheless, the peak E-field EF on the other side (E_{max2}) is still larger than the maximum EF observed in Case I of Fig. 2(a), as the average dielectric constant in the small pore is still higher than that on the top surface. We proceed to conduct a further study on the NP dimer, which has been demonstrated that the biomedical detection sensitivity to be increased by several times compared to isolated metal NPs due to the strong field confinement. A NP dimer is constructed inside the pore as shown in Fig. 2(c), which consists of two NPs with 24-nm diameter and a gap size of 2 nm. Compared with the E-field of the same Ag NP dimer on a glass substrate, the maximum EF inside the pore increases from 49× to 235×, which gives an improvement factor of 4.8×. Relatively large redshifts of resonant wavelengths from glass substrates to diatom frustules were observed: for a single Ag NP, the resonant wavelength shifts from 391 nm to 40 6nm due to the change of the dielectric surrounding. For a NP dimer, the resonant wavelength shifts from 418 nm to 433 nm. The increase of the redshift magnitude of the LSPs for a dimer is attributed to the enhancement of the particle near-field coupling.

3. EXPERIMENTAL RESULTS

3.1 Sample Preparation

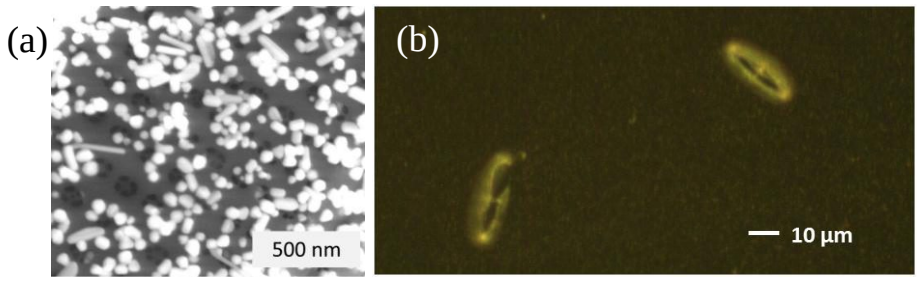

Fig.3 (a) SEM picture of Ag NPs self-assembled on the diatom frustule; (b) Dark-field image of self-assembled Ag NPs on diatoms frustules and on glass substrates.

The preparation of diatom frustules can be found in our previous work [10]. For the Ag nanoparticles synthesis, the colloidal was prepared by the Lee and Mesel Method [11]. The diatom-coated substrates were modified with aminopropyltriethoxylsilane (APTES) to promote NP adhesion [12]. After that, the substrates were then exposed to an Ag colloidal suspension for 12 h to deposit the Ag NPs onto the frustules and the underlying substrate. After being

removed from the NP solution, the sample was rinsed with deionized water and dried with high-purity nitrogen. The representative SEM image in Fig. 3(a) shows the densely assembled Ag NPs on the diatom frustule. Fig. 3(b) shows a dark-field image of self-assembled Ag NPs on diatom frustules demonstrating stronger optical scattering compared to the self-assembled Ag NPs on the surrounding glass substrate.

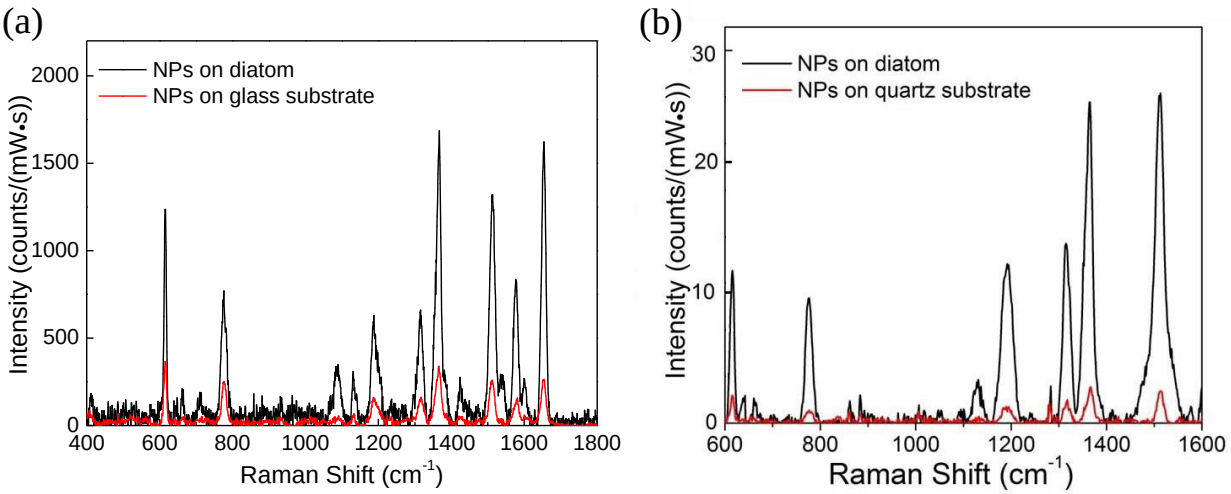

Figure 4 (a) Single point SERS measurement (Under 532 nm excitation) of 1μM R6G coated on Ag NPs-on-diatom (black) and Ag NPs-on-glass (red). During the measurement, the excitation power was set at 1.2 mW and integration time was 1 second. (b)Single point SERS measurement (Under 785 nm excitation) of 100 μM R6G coated on Ag NPs-on-diatom (black) and Ag NPs-on-quartz (red). During the measurement, the integration time was 60 second and the grating groove density was set at 300/mm. The excitation power was 2.1 mW.

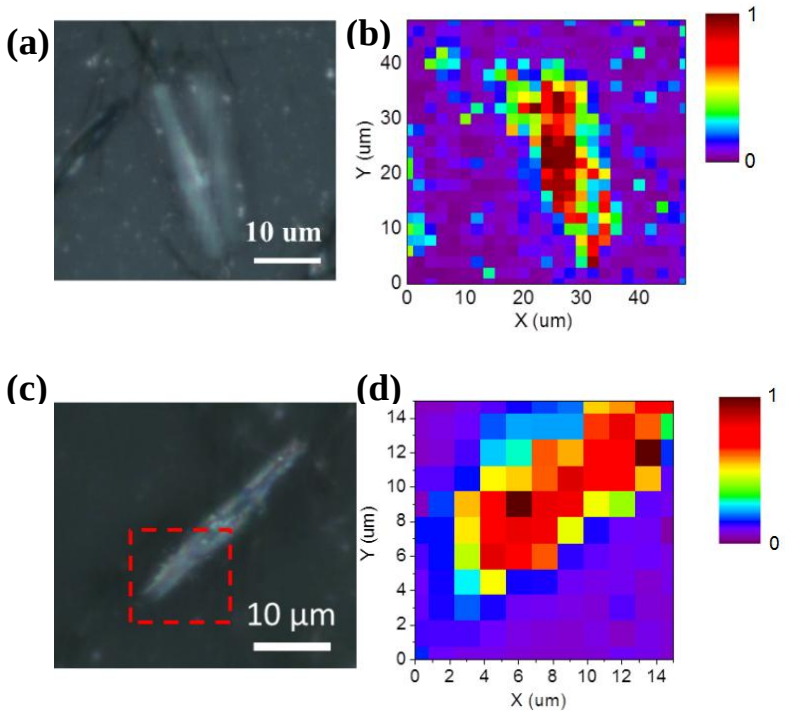

Figure 5. (a) Optical image of the sensing area scanned for SERS measurement under 532 nm excitation, and (b) Mapping of Raman signal intensity at 1368 cm^{-1}. During measurement under the 532 nm excitation, the excitation power was set at 1.2 mW and integration time was 1 second. (c) Optical image of the area scanned for SERS measurement under 785 nm excitation, and (d) Map of Raman signal intensity at 1368 cm^{-1}. During the measurement under 785 nm excitation, the integration time was 60 second and the grating groove density was set at 300/mm. The excitation power was 2.1 mW.

We experimentally investigated diatom biosilica with self-assembled Ag NPs as a platform for SERS detection of Rhodamine 6G (R6G) molecules using the excitation light at molecular resonance wavelength (532 nm) and nonresonance wavelength (785 nm), respectively. In our SERS measurement, R6G molecules in ethanol were drop-coated on the glass substrate with diatom frustules and then evaporated to dryness. SERS microscopy was performed using a Horiba Jobin-Yvon HR800 confocal Raman spectrometer equipped with a diode laser through a notch filter. During the measurement, the confocal pin-hole size was set at 100 μm. A 50× objective lens (NA = 0.75) was used to focus the excitation light to a 2 μm spot totally within a single diatom frustule for each spectrum acquisition. Raman signals were detected by a Synapse charge-coupled device (CCD) detector. Fig. 4(a) shows the single-point resonance (532 nm) SERS signals of 1μM R6G measured on the flat glass substrate and on the diatom frustule respectively. SERS signals of the NPs-on-diatom structure show 3.6-6.2× enhancement compared with that on the NPs-on-glass substrate for major R6G Raman peaks at 614 cm^{-1}, 1368 cm^{-1}, 1511 cm^{-1}, 1578 cm^{-1} and 1651 cm^{-1}. The additional enhancement of Raman signals is attributed to the enhanced LSPs due to the presence of the diatom frustule. Furthermore, SERS spectra were recorded using 785 nm excitation wavelength to avoid a complex interference of molecular resonance Raman scattering effect since the excitation energy of 785 nm is away from the electronic absorption band of R6G, which results in nonresonance Raman scattering. Due to the fact that the glass substrate displays strong florescence background under the 785 nm wavelength excitation, diatom frustules in aqueous solution were drop-coated on non-florescent quartz substrate for the measurement. The diatom frustules were annealed at 425 ˚C in air for 1 hour in order to improve the adhesion to the quartz substrate. The fabrication process of self-assembled NPs onto a diatom-coated quartz substrate is identical to the diatom-coated glass substrate. Fig. 4(b) shows the nonresonance SERS spectra under the 785 nm excitation light from a diode laser. The SERS spectra indicates that the Raman signal intensity is enhanced by 8.7-13.3× on the diatom frustule compared with the flat quartz substrate for the Raman bands of 776 cm^{-1}, 1183 cm^{-1}, 1315 cm^{-1}, 1368 cm^{-1}, and 1511 cm^{-1}. The larger additional enhancement factors from diatom frustules to the R6G Raman signals under nonresonance condition compared with resonance condition can be explained by the difference between resonance and nonresonance Raman scattering by surface plasmons. Resonance Raman process is subjected to quenching effect, where an additional loss is introduced for the energy stored in coherent oscillations of molecular dipoles at the excitation wavelengths in the presence of LSP enhancement and GMR enhancement [13]. Compared with resonance Raman process which limits the attainable enhancement, such quenching effect is absent in normal nonresonance Raman scattering.

By mapping a large area of the substrate which includes a diatom frustule as well as some flat glass surface, we are able to investigate the effect of the photonic-crystal-like structure of diatom frustule on SERS signal intensity. For the SERS mapping measurement under 532 nm excitation, a total of 625 SERS spectra were acquired within the scanning range of 50 μm×50 μm that is divided into an acquisition area of 25 × 25 grids, as shown in Fig. 5(a) and Fig. 5(b). The SERS mapping results of the intensity of 1368 cm^{-1} Raman peak exhibit a pattern of increased signal intensity which correlates with the shape of the diatom frustule that is observed in the corresponding optical image. The presence of the diatom photonic structures results in an average SERS enhancement factor of 4.3× compared to that on the flat glass substrate. The enhancement factor was strongly correlated to the enhanced electric field around the Ag NPs due to the GMRs of the photonic crystal structure. For the SERS mapping measurement under 785 nm excitation, an area of 15 μm×15 μm in Fig. 5(c) was scanned to generate a map in Fig. 5(d). The average measured SERS signal intensity for the NPs-on-diatom area shows an average signal enhancement of 9.2× compared to quartz substrate. Such enhancement factor for nonresonance SERS is more desirable for biosensing application as fluorescence interference can be avoided compared with resonance SERS.

4. CONCLUSION

In conclusion, we have demonstrated that the guided-mode resonances of diatom frustules can effectively couple with the localized surface plasmons of the Ag NPs, which will increase the average enhancement factor of SERS sensors. An additional enhancement factor of the SERS signals of 4-6× was observed for resonance condition. Under nonresonance condition, the Raman enhancement factor of 9-12× was obtained. Such NPs-on-diatom SERS substrate will have significant potentials in chemical and biochemical diagnostics, pathogen detection, and environmental protection.

REFERENCES

[1] Anker, J. N., Hall, W. P., Lyandres, O., Shah, N. C., Zhao, J., and Van Duyne, R. P., "Biosensing with plasmonic nanosensors," Nat. Mater. 7, 442-453 (2008).

[2] Brolo, A. G., "Plasmonics for future biosensors," Nat. Photonics 6, 709-713 (2012)

[3] Homola, J. , Yeea, S. S., and Gauglitzb, G., "Surface Plasmon Resonance Sensors: Review," Sens. Actuators, B, 54, 3-15, (1999).

[4] Xu, X., Hasan, D., Wang, L., Chakravarty, S., Chen, R. T., Fan, D. L., and Wang, A. X., "Guided-mode-resonance-coupled plasmonic-active SiO_2 nanotubes for surface enhanced Raman spectroscopy, Appl. Phys. Lett. 100, 191114-1-191114-5(2012).

[5] White, I. M., Gohring, J., and Fan, X.,"SERS-based detection in an optofluidic ring resonator platform." Opt. Exp., 15(25), 17433-17442(2007).

[6] Hu, M., Fattal, D., Li, J., Li, X., Li, Z., and Williams, R. S., "Optical properties of sub-wavelength dielectric gratings and their application for surface-enhanced Raman scattering," Appl. Phys. A, 105(2), 261-266(2011).

[7] Gordon, R., Losic, D., Tiffany, M. A., Nagy, S. S., and Sterrenburg, F. A., "The glass menagerie: diatoms for novel applications in nanotechnology," Trends Biotechnol., 27, 116-127(2009).

[8] Jeffryes, C., Campbell, J., Li, H., Jiao, J., and Rorrer, G., "The potential of diatom nanobiotechnology for applications in solar cells, batteries, and electroluminescent devices," Energy Environ. Sci. 4, 3930-3941(2011).

[9] Jeffryes, C., Solanki, R., Rangineni, Y., Wang, W., Chang, C. H., and Rorrer, G. L., "Electro-luminescence and photoluminescence from nanostructured diatom frustules containing metabolically inserted Germanium," Adv. Mater., 20, 2633-2637(2008).

[10] Ren, F., Campbell, J., Wang, X., Rorrer, G. L., and Wang, A. X., "Enhancing surface plasmon resonances of metallic nanoparticles by diatom biosilica," Opt. Exp., 21(13), 15308-15313(2013).

[11] Lee, P. C., and Meisel, D. J., "Adsorption and surface-enhanced Raman of dyes on silver and gold sols," Phys. Chem., 86, 3391-3395(1982).

[12] Liu, S., Zhu, T., Hua R., and Liu, Z., "Evaporation-induced self-assembly of gold nanoparticles into a highly organized two-dimensional array," Phys. Chem. Chem. Phys., 4, 6059-6062(2002).

[13] Sun, G., and Khurgin, J. B., "Origin of giant difference between fluorescence, resonance, and nonresonance Raman scattering enhancement by surface plasmons." Phys. Rev. A, 85(6), 063410(2012).